A space-time-frequency dictionary for sparse cortical source localization

Gundars Korats, Steven Le Cam, Radu Ranta, Valérie Louis-Dorr

▶ **To cite this version:**

Gundars Korats, Steven Le Cam, Radu Ranta, Valérie Louis-Dorr. A space-time-frequency dictionary for sparse cortical source localization. IEEE Transactions on Biomedical Engineering, 2016, 63 (9), pp.1966-1973. 10.1109/TBME.2015.2508675 . hal-01259897

HAL Id: hal-01259897
https://hal.science/hal-01259897

Submitted on 21 Jan 2016

HAL is a multi-disciplinary open access archive for the deposit and dissemination of scientific research documents, whether they are published or not. The documents may come from teaching and research institutions in France or abroad, or from public or private research centers.

L'archive ouverte pluridisciplinaire **HAL**, est destinée au dépôt et à la diffusion de documents scientifiques de niveau recherche, publiés ou non, émanant des établissements d'enseignement et de recherche français ou étrangers, des laboratoires publics ou privés.

A space-time-frequency dictionary for sparse cortical source localization

Gundars Korats[1,2,⋆], Steven Le Cam[1], Radu Ranta[1] and Valérie Louis-Dorr[1]

Abstract

Cortical source imaging aims at identifying activated cortical areas on the surface of the cortex from the raw EEG data. This problem is ill-posed, the number of channels being very low compared to the number of possible source positions. In some realistic physiological situations, the active areas are sparse in space and of short time durations, and the amount of spatio-temporal data to carry the inversion is then limited. In this work, we propose an original data driven space-time-frequency dictionary which takes into account simultaneously both spatial and time-frequency sparseness while preserving smoothness in the time-frequency (*i.e.*, non-stationary smooth time courses in sparse locations). Based moreover on these assumptions, we take benefit of the Matching Pursuit (MP) framework for selecting the most relevant atoms in this highly redundant dictionary. We apply two recent MP algorithms, Single Best Replacement (SBR) and Source Deflated Matching Pursuit (SDMP), and we compare the results using a spatial dictionary and the proposed Spatial-Time-Frequency (STF) dictionary to demonstrate the improvements of our multidimensional approach. We also provide comparison using well established inversion methods, FOCUSS and RAP-MUSIC, analysing performances under different degrees of non-stationarity and signal to noise ratio.

Index Terms

EEG, Sparse Source Localization, Time-frequency decomposition, Wavelets, Matching Pursuit, Single Best Replacement, Source Deflated Matching Pursuit

I. Introduction

Synchronous firing of large neural populations in the brain can be measured on the scalp using EEG sensors. These potentials appear to be generated by strong cortical sources involving large patches of neighbouring neurons. Due to the complex nature of brain sources, and to the smearing effect of the skull, the signal-to-noise ratio is generally low. In addition, the activities of different brain areas might be temporally synchronized, both during normal and pathological functioning, leading to linearly dependent measurements polluted with artefact sources such as ocular or muscular movements.

In order to localize the activated brain sources within the brain volume or on the cortical surface, an inverse problem has to be solved. In general, this implies the resolution of a high-dimensional and badly conditioned linear problem, with an infinite number of solutions, thus needing regularization. This can be done either on unique time instants or on time windows, the latter solution naturally imposing a kind of spatial regularization to preserve a spatial coherence of the source location in time.

Two main families of source localization methods exists in the literature. The first one includes the equivalent current dipole (ECD) fitting and the derived parametric methods that yield an estimation of dipole location, orientation and amplitude [1], [2]. Applied on single time instants, it might yield discontinuous solutions, "jumping" from one location to another between two consecutive time instants (moving dipole solution). A regularization is introduced by imposing fixed dipole positions and/or orientations on a given time window [3].

The second family consists in the linear distributed approaches (LD), based on distributed source models discretizing the source space into point source locations in the brain volume. The solution is computed by minimizing a cost function such as overall minimum power or minimum current [4]–[6]. Among the existing regularization techniques, a family of approach comes rather close to the ECD methods by imposing sparsity, *i.e.*, aiming to find a solution which involves a minimal number of (strong enough) active brain sources, possibly contaminated by background activity (assumed as noise). Sparse source localization has gained more and more attention in the last few years, since it is now generally assumed that only a limited number of cortical areas are indeed active within short windows of time. The scalp measurements are summed up using few point sources, each standing for the mean activation of a close surrounding area, and providing easy interpretable visual results at destination of clinicians and neurophysiologists. Besides, such approaches greatly simplify the analysis of the underlying brain networks, where each identified point source can be considered as a node of a graph of connected structures. The identification of the interactions between particular cortical areas within networks is widely believed to be a key stone for the understanding of the functional (memorization, cognition, *etc.*) as well as the pathological organization of the brain [7]–[10].

A recent block-sparse method called source deflation matching pursuit (SDMP) [11] was developed to estimate dipole locations and orientations for every time instant, being thus an LD equivalent of the ECD moving dipole approach. Among

[1] All authors are with the Université de Lorraine, CRAN, UMR 7039, 54500 Vandoeuvre les Nancy, France and with the CNRS, CRAN, UMR 7039, France gundars.korats at univ-lorraine.fr
[2] Gundars Korats is also with Ventspils University College, 101 Inzenieru iela, LV-3601, Ventspils, Latvia gundars.korats@gmail.com
⋆ Corresponding author
Supported by the Latvian National Research Programme "The next generation of information and communication technologies" (NextIT).

the sparse distributed models coming close to the ECD approaches on time windows, two of the most well-known methods are MUltiple SIgnal Classification (MUSIC) and its recursive extension RAP-MUSIC [12]. Both algorithms scan single-dipole position all over the head volume and compute their projections onto the estimated signal subspace to identify the source locations.

A common characteristic of time-window based methods is the assumption of stationarity, at least spatially (for ECD approaches), but also temporally (for statistic based MUSIC methods). However the dynamics of the sources are most of the time transient and are known to lie within particular time-frequency subspaces. It is in particular the case when studying the dynamic of epileptic seizures [13] or of steady-state evoked potential [14]. In this context of MP localization, the only approach to our knowledge taking benefit of such time-frequency features in the EEG signal was proposed by [15] as a sparse representation of EEG/MEG data using spatio-temporal atoms. Each atom is formed as a combination of wavelet coefficients of scalp observations together with the forward model (lead-field).

Inspired by this work, we propose in this paper an optimal time-frequency-space dictionary to be combined with efficient optimization approaches ensuring sparsity. Unlike in [16], where we assumed stationary data and we extracted a PCA based time dictionary, we compute a wavelet dictionary by applying a threshold strategy on the wavelet coefficients [17], [18]. We then introduce the spatial constraint by forming spatio-temporal atoms using a realistic forward BEM model [19]. The stationarity constraint is indeed relaxed, but we still enforce a spatial coherence on short time windows. We keep the size of the dictionary reasonable by extracting the temporal atoms from the data, and the decomposition is directly carried out in the wavelet domain, thus resulting in an acceptable computational burden. We evaluate the advantage of using such dictionaries on two recent MP algorithms: the Single Best Replacement (SBR) and the Source Deflated Matching Pursuit (SDMP), that we modified to adapt to the proposed dictionary.

The structure of the paper is following: in section II-A we provide the forward model to invert. The principles of sparse approximation are then introduced in section II-B, along with brief overviews of both SBR and SDMP algorithms. Section II-C1 explains the details of the wavelet-based dictionary design, which is used to construct the complete space-time-frequency dictionary as presented in section II-C2. Next, in II-D, the concept of sparse space-time-frequency approximation is explained and the pseudo-code of the MP-based localization methods is provided. In section III we provide details of simulation set-up and performance measures. Finally, we discuss the results (section III-C) and demonstrate the advantages as well as the drawbacks of using such dictionaries. We also emphasize the strengths and weakness of SBR and SDMP as functions of the number of underlying sources, the non-stationarity of the data and the power of the noise.

II. Methods

A. Forward model

Consider the following classical forward model:

$$\mathbf{V} = \mathbf{AS} + \mathbf{E} \tag{1}$$

where scalp EEG recordings $\mathbf{V}_{N\times T}$ (N the number of EEG channels and T the number of time samples) are a linear combination of M time-varying dipole magnitudes $\mathbf{S}_{M\times T}$ driven by the lead-field matrix $\mathbf{A}_{N\times M}$. Each column of this matrix corresponds to the projection of a unit amplitude dipole, considered here orthogonal to the inner skull surface (this is a common assumption in EEG problems, based in the parallel organization of the cortical pyramidal neurons). An important characteristic of the $\mathbf{A}$ matrix is that its neighbouring columns are highly correlated among them, as they stand for close spatial positions with similar orientations. Finally the matrix $\mathbf{E}$ denotes noise with the same dimensions as $\mathbf{V}$.

B. Sparse approximation

Sparse signal decomposition of $\mathbf{V}$ requires finding a limited number of elements from the dictionary $\mathbf{A}$ such that their weighted sum best describes the observation data $\mathbf{V}$. The popularity of sparse approximation algorithms relies on their ability to provide efficient sparse approximations of a signal for under-determined problems [20].

In the spatial domain, sparse signal approximation of some arbitrary chosen data vector $\mathbf{V}_t$ (one time instance of multichannel data) can be formulated as the minimization of the penalized least-square cost function:

$$\min_{\mathbf{S}_t} \ \mathcal{J}(\mathbf{S}_t, \lambda) = ||\mathbf{V}_t - \mathbf{AS}_t||_2^2 + \lambda||\mathbf{S}_t||_0 \tag{2}$$

where the l_0 pseudo-norm of the weight column vector $\mathbf{S}_t$, defined as the number of its non-zero entries, is lower than a given number $k \ll M$. By this equation we are trying to find a sparse representation of the data (parametrized by the sparsity penalty parameter λ) meaning that only a few sources are active at a time. The l_0 norm is a natural measure of sparsity but it leads to optimization related problem, which is NP-complete. This means that all possible combinations of the dictionary elements should be considered, yielding exhaustive search algorithms with high computational cost.

Greedy iterative approaches such as Matching Pursuit (MP) provide the easiest way to find an approximate solution of the original l_0 pseudo-norm problem by finding g dictionary elements and their corresponding weighting coefficients, *i.e.*, non

zero elements of $\mathbf{S}_t$ in (2). The approximation of the observation $\mathbf{V}_t$ found by MP can be written as the following linear expansion [21], [22]:

$$\mathbf{V}_t = \sum_{n=1}^{g} \mathbf{a}_n s_n \tag{3}$$

with $\mathbf{a}_n$ the n-th column of the leadfield matrix $\mathbf{A}$ and s_n its weight, corresponding to the amplitude of the n-th dipole. Matching pursuit suffers from the drawback that a particular atom can be picked multiple times. This issue is being solved in Orthogonal Matching Pursuit (OMP) proposed in [23] where each atom can be picked only once. A more effective and also more computationally expensive method is Orthogonal Least Squares (OLS), where in each iteration step a least squares problem is solved instead of a simple product calculation as it is in the standard MP case. Nevertheless, for highly correlated dictionaries, OLS together with OMP does not guarantee to find an optimal solution [20].

An improved way to solve the equation (2) is to use forward-backward greedy algorithms, as for example proposed by Zhang in [24], which is a forward-backward OMP extension. The advantage comes from its ability to eliminate the errors made in previous iterations. The limitation of this method is that it works well only if the basis functions are nearly or completely orthogonal.

1) Sparse approximation using SBR: As mentioned in section II-A, in our case the data are noisy and dictionary elements can be highly correlated. A recent method dealing with this situation is the Single Best Replacement (SBR) algorithm proposed in [20], where equation (2) is seen as a subset or feature selection problem. SBR is an Ordinary Least Squares (OLS) forward-backward extension based on successive updates of the sparse signal support (dictionary element indices) by one element: at each step, the support Q is updated (insert "$\cup$" a new element with index ij inside the support or remove "$\setminus$" an existing support element) [20]. The forward-backward rule shown in equation (4) ensures that only the most significant columns of $\mathbf{A}$ weighted by $\mathbf{S}_t$ are chosen.

$$Q \bullet i = \begin{cases} Q \cup \{i\} & \text{if} \quad i \notin Q \\ Q \setminus \{i\} & \text{otherwise} \end{cases} \tag{4}$$

This leads to the construction of an *active set* $\mathbf{A}_Q$, where Q contains the selected column indexes (active source locations). Basically SBR is designed to solve discrete NP-complete problem and, in fact, is a deterministic descent algorithm that minimizes $\mathcal{J}$ from (2) with a fixed parameter λ. Each iteration is based on the computation of $Q \bullet i$ for all i and the selection of the replacement $Q \bullet l$ yielding the minimal value of $\mathcal{J}_{Q \bullet i}(\mathbf{S}_t, \lambda)$ [20]:

$$l \in \underset{i \in \{1,\ldots,n\}}{\arg\min} \; \mathcal{J}_{Q \bullet i}(\mathbf{S}_t, \lambda) \tag{5}$$

Then if $\mathcal{J}_{Q \bullet l}(\lambda) < \mathcal{J}_Q(\lambda)$, the subset Q is updated with the new element $Q = Q \bullet l$. Finally SBR stops when no replacement decreases the cost function or some predefined stopping condition is met, e.g. the residual is significantly small or the maximum size of the subset is reached. If $\lambda > 0$, SBR stops after a finite number of iterations.

2) Sparse approximation using SDMP: The SDMP algorithm, as presented in [11], start by initializing a set of eligible source positions using a BMP or ORMP algorithm. The number of sources has to be given as a prior and can be extracted from a noise/source subspace analysis like in the case of the RAP-MUSIC algorithm.

In a second step, each of the selected source positions p are iteratively reconsidered along with the set of unselected positions. This is done by suppressing from both the data and the lead-field the contributions of the selected positions minus the current refined position p, using the following projection matrix:

$$\mathbf{P}_p^{\perp} = \mathbf{I} - \mathbf{A}_{\setminus p}[(\mathbf{A}_{\setminus p})^T \mathbf{A}_{\setminus p}]^{-1} (\mathbf{A}_{\setminus p})^T. \tag{6}$$

$\mathbf{A}_{\setminus p}$ being the current set of selected lead-field columns minus the one corresponding to the position p. It has to be emphasized that we only consider fixed orientation of the dipoles orthogonal to the cortical surface, thus we do not consider the post re-estimation of the dipoles orientation/moment (the Source Deflated MUSIC (SDMUSIC) algorithm) described in the paper of Wu *et al.* [11].

C. Dictionary design

When it comes to brain source localization, MP methods are usually applied using the columns of the lead-field as the dictionary, without considering temporal constraints. Imposing simultaneously temporal shapes and spatial patterns will help in regularizing the localization problem. We first present how time-frequency atoms are extracted from the data, and we then combine them to the spatial lead-field atoms to form our Spatial-Time-Frequency (STF) dictionary.

1) Time-frequency dictionary: Using Principal Component Analysis (PCA), the K principal components can be extracted from the data, forming a basis of the source space in the time domain. Under the assumption of stationarity, the basis vectors $\mathbf{S}_{PCA}$ can be used directly as a temporal dictionary $\mathbf{D}_{PCA}$ [16]. A common criteria for solving this problem is the MDL (minimum description length) rule, as proposed and explained in [25], [26]. To avoid such criteria, we thus address in this work the more general case of non-stationary sources by constructing our dictionary in the wavelet domain, more precisely by using orthogonal real wavelets. The advantage of such approach is that wavelet coefficients can be used individually to efficiently capture specific time-frequency characteristics of the sources, while preserving smoothness. Indeed, the compression ability of the wavelets leads to sparse time-frequency representations of the signal of interest and thus to less computationally expensive solutions. Moreover, fast algorithms exist for both wavelet decomposition and reconstruction. In the following, we assume that every signal of length T is decomposed up to the depth J (the number of detail scales) and thus that on every scale j we have $T/2^j$ wavelet coefficients.

To generate sparse wavelet dictionary $\mathbf{D}_w$, we apply the wavelet threshold directly to the noisy data. In fact the projection of the original data on its principal components is not needed as the denoising is done by wavelets. This allows us to avoid the major difficulty of selecting the most significant eigenvalues.

A lot of thresholding techniques exist in the literature (see for example [27] for a review). We tested only the classical solutions proposed by Donoho and Johnstone [28] (universal and SURE thresholding), as well as a combination of them, suggested under the name of hysteresis thresholding in [29] and slightly modified here, as explained further.

By its construction (aiming to preserve as much signal as possible even if some noise remains present), the SURE threshold is rather low and preserves a lot of coefficients, increasing thus the size of the wavelet dictionary. On the other hand, the universal threshold aims to completely eliminate the noise and keeps only the strong coefficients with big amplitudes. It yields a very sparse temporal approximation, in principle less accurate than the SURE threshold but almost noise-free (for details see [27] and [28]).

Hysteresis threshold aims to exploit the advantages of both: it preserves all the coefficients selected by the universal threshold and adds all the SURE-selected coefficients that are connected, in the time-frequency plane, with one of the universal coefficients. Taking into account that each universal coefficient is also preserved by SURE threshold, this technique simply consists in labeling the connected components in a 2-dimensional binary image. At first we label each isolated coefficient or isolated connected group of coefficients in time-frequency scale. Once binary images of both universal and SURE thresholds are labeled, one can detect the hysteresis coefficients by a simple subtraction where each individual labeled coefficient group from universal threshold is being subtracted from the SURE labeled coefficients. Those groups of coefficient in the SURE labeled image impacted by the subtraction are preserved as Hysteresis coefficients (see Fig. 1).

Let $\mathbf{v}_w^i$ be the vector of "clean" wavelet coefficients after applying wavelet threshold to the noisy data channel $\mathbf{v}^i$. Depending on the threshold, this vector will be more or less sparse. Each non-null coefficient represents the time-frequency support of a wavelet coding a significant feature of the analysed signal $\mathbf{v}^i$, and we can construct a binary mask corresponding to these supports (see Fig. 1). A logical OR among all masks (obtained for all channels) yields a complete mask, where the non-null elements designate all the necessary wavelets for the approximate noise free reconstruction of the complete measurements matrix $\mathbf{V}$. Each individual coefficient corresponds in fact to a time-frequency dictionary element $w_{p_j}^j$, which is a wavelet on scale (frequency band) j at time-shift p_j. The complete time-frequency dictionary is then the family of selected wavelets $\mathbf{D}_w = \{w_{p_j}^j\}$, with scales $j \in \{1, \cdots, J\}$ and time shifts $p_j \in \{1, \cdots, T/2^j\}$.

2) STF dictionary: The obtained time-frequency dictionary $\mathbf{D}_w$ imposes time-frequency constraints which needs to be combined with the spatial dictionary formed by the columns of the lead-field matrix $\mathbf{A}$, before it can be used for minimizing the criterion of equation (2). Let this space-time-frequency dictionary be $\mathbf{H} = \{\mathbf{h}_{ip_jj}\}$, where each element $\mathbf{h}_{ip_jj}$ of dimension $N \times T^j$ (T^j being the support size of the wavelets on scale j) is a rank one matrix obtained by:

$$\mathbf{h}_{ip_jj} = \mathbf{a}_i w_{p_j}^j \tag{7}$$

In the EEG application addressed in this work, $\mathbf{H}$ can be seen as a set of time-varying scalp-maps shifted in time and frequency.

D. Spatio-Temporal Matching Pursuit

The observation data are approximated with a weighted sum of the $\{\mathbf{h}_{ip_jj}\}$ dictionary elements:

$$\hat{\mathbf{V}} = \sum_i \sum_{p_j} \sum_j b_{ip_jj} \mathbf{h}_{ip_jj} \tag{8}$$

where b_{ip_jj} are scalar amplitudes/weights which can be grouped in a vector $\mathbf{b}$. The minimization problem for SBR is formulated as follows:

$$min_{\mathbf{b}} \ \{\mathcal{J}(\mathbf{b}, \lambda) = ||\mathbf{V} - \hat{\mathbf{V}}||_2^2 + \lambda ||\mathbf{b}||_0\} \tag{9}$$

with the term $\lambda||\mathbf{b}||_0$ balancing the number of nonzero weighting elements in $\mathbf{b}$ (*i.e.*, selected rank one matrices $\mathbf{h}_{ip_jj}$), regularizing the sparsity in simultaneously in space and time-frequency.

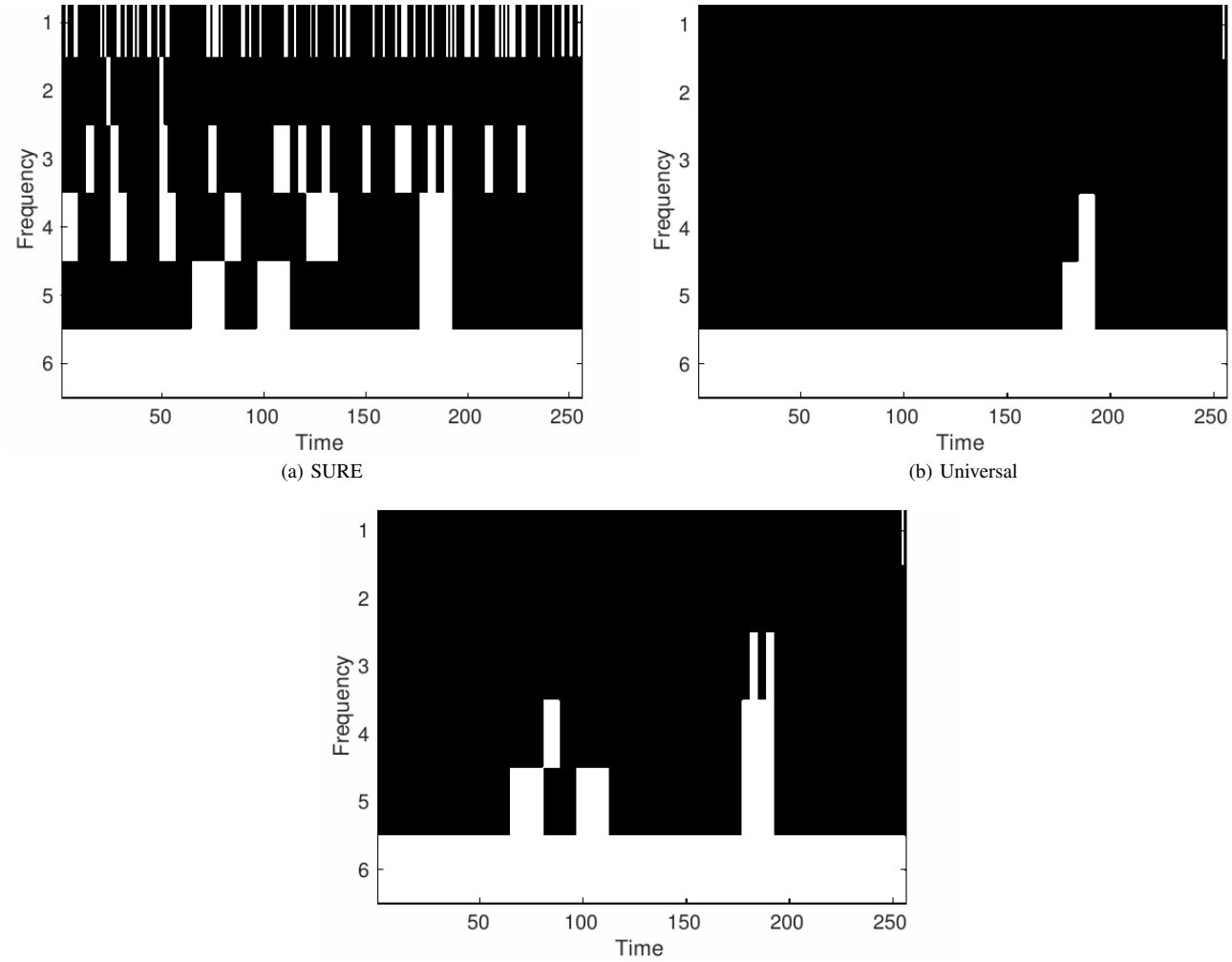

(a) SURE

(b) Universal

(c) Hysteresis

Fig. 1: Binary image of coefficients obtained using (a) SURE and (b) universal wavelet threshold. The SURE coefficients connected to the universal group of coefficients are preserved to give the (c) Hysteresis wavelet threshold. In all images the horizontal axis represents time, and the vertical axis represents the scale (frequency band).

The choice of an optimal sparsity parameter λ is a difficult task. As this parameter is used for selecting the significant atoms explaining the signal of interest (source projections) but not the noise components, it should be proportional to a fraction of the noise energy $\mathcal{E}_n$. A more detailed analysis of the influence of this parameter is given in the results section.

The general structure of our proposed Spatio-Temporal SBR (ST_SBR) decomposition procedure is shown in **Algorithm 1**.

Algorithm 1 Spatio-Temporal SBR

1: **procedure** ST_SBR()
2: **Give or estimate the noise energy** $\mathcal{E}_n$
3: **Compute** λ**:** Equation (16).
4: **Construct D**: Wavelet threshold (section II-C1).
5: **Compute H**: Equation (7).
6: **Decompose data**: Solve equation (9) using SBR.
7: **end procedure**

In case of SDMP the number of sources N_s is assumed to be known or estimated and thus writes:

$$min||\mathbf{V} - \sum_{i}^{N_s} \sum_{p_j} \sum_{j} b_{ip_jj} \mathbf{h}_{ip_jj}||_2^2 \tag{10}$$

The residual is minimized considering the given fixed number of locations for each individual wavelet support. Similarly as the estimation of the parameter λ in the case of the SBR algorithm, the estimation of the number of sources is difficult. Both issues are actually connected because they both rely on a source/noise subspace analysis and they will be analyzed in the Results section. The global structure of the algorithm is given in **Algorithm 2**.

Algorithm 2 Spatio-Temporal SDMP

1: **procedure** ST_SDMP()
2: **Give or estimate** N_s
3: **Construct D**: Wavelet threshold (section II-C1).
4: **Compute H**: Equation (7).
5: **Decompose data**: Solve equation (10) using SDMP.
6: **end procedure**

III. Simulations and results

A. Data simulation

The aim of this work is to evaluate the performance of cortical source localization and data reconstruction in the context of non-stationary sources, by use of the proposed spatio-temporal dictionary. We start by simulating a quasi-continuous brain surface by a dense discrete layer of 1200 dipoles placed $5mm$ under the inner skull surface. The dipoles have fixed orientation normal to the inner skull layer. For realistic simulations, we randomly choose a subset of 8 or 16 dipoles to be active among the 1200 positions. We assign real time-courses to the selected dipoles, taken from an intracranial Stereo-EEG (SEEG) recording of an epileptic patient. Namely, we choose 2 seconds (512 points using 256Hz sampling frequency) of 8 or 16 SEEG signals to simulate the activated dipoles. Non-stationarity is obtained by considering that each of these dipoles is active during only one epoch within these 2 seconds, with two simultaneous active sources per epoch, *i.e.*, 4 (respectively 8) epochs of 500ms (respectively 250ms) for the 8 (respectively 16) dipoles case. We use further a realistic three layer (*Colin27*) head model extracted from BRAINSTORM [19]. Potentials at 128 simulated BIOSEMI scalp sensors are computed using a BEM forward model from the Helsinki toolbox [30]. Physiological background activity was simulated by adding spatially colored Gaussian noise (random co+variance matrix), with two signal to noise ratios (SNR) of 10dB and 3dB. We provide mean results over 100 simulations for each of the simulated configurations.

Fig.2 shows and example of such non-stationary set-up for the 8 sources configuration.

B. Performance measure

In the following, we will consider as a True Positive (TP) an estimated dipole located within $1cm$ from a simulated dipole. All estimated components that are farther than $1cm$ are False Positives (FP).

We are interested in both data reconstruction quality and localization accuracy. A Goodness-of-fit (GOF) is used to measure the quality of scalp potential reconstruction:

$$\mathrm{GOF} = 1 - \frac{||\mathbf{V}_{clean} - \hat{\mathbf{V}}||^2}{||\mathbf{V}_{clean}||^2} \tag{11}$$

where $\mathbf{V}_{clean}$ corresponds to the noise-free source projection on the scalp, whereas $\hat{\mathbf{V}}$ stands for the reconstructed scalp potentials. We also compute $\mathrm{GOF_s}$ replacing in (11) $\hat{\mathbf{V}}$ by $\mathbf{V}_{TP}$, that is the reconstruction of the scalp potentials using only TP dipoles. This is done in order to evaluate if the resulting TP indeed explain the original data. The GOF is far from a sufficient statistic to evaluate the accuracy of the source reconstruction. Indeed the problem is under-determined and several configuration of sources might lead to the same scalp map. We thus propose additional criteria assessing the quality of the results.

The Distance Localization Error (DLE), as proposed in [31], gives an estimate of the localization accuracy taking into account both the missed simulated sources (FN) as well as the introduction of spurious sources (FP):

$$\mathrm{DLE} = \frac{1}{2Q}\sum_{k\in I} min_{l\in\hat{I}}||r_k - r_l|| + \frac{1}{2\hat{Q}}\sum_{l\in\hat{I}} min_{k\in I}||r_k - r_l|| \tag{12}$$

Here, the I and $\hat{I}$ denote the original and estimated sets of dipole index. r_k denotes the position of the *k*-th simulated source while r_l denotes the position of the *l*-th estimated dipole. This DLE equally penalize too sparse solutions with missed sources (first member of the criterion), as well as less sparse solutions introducing spurious dipoles far from the true sources (second member of the criterion), and this even when the whole set of true sources are indeed localized. This statistic must be read along with the rate of false discovery (FDR):

$$\mathrm{FDR} = \frac{\mathrm{FP}}{(\mathrm{TP} + \mathrm{FP})} \tag{13}$$

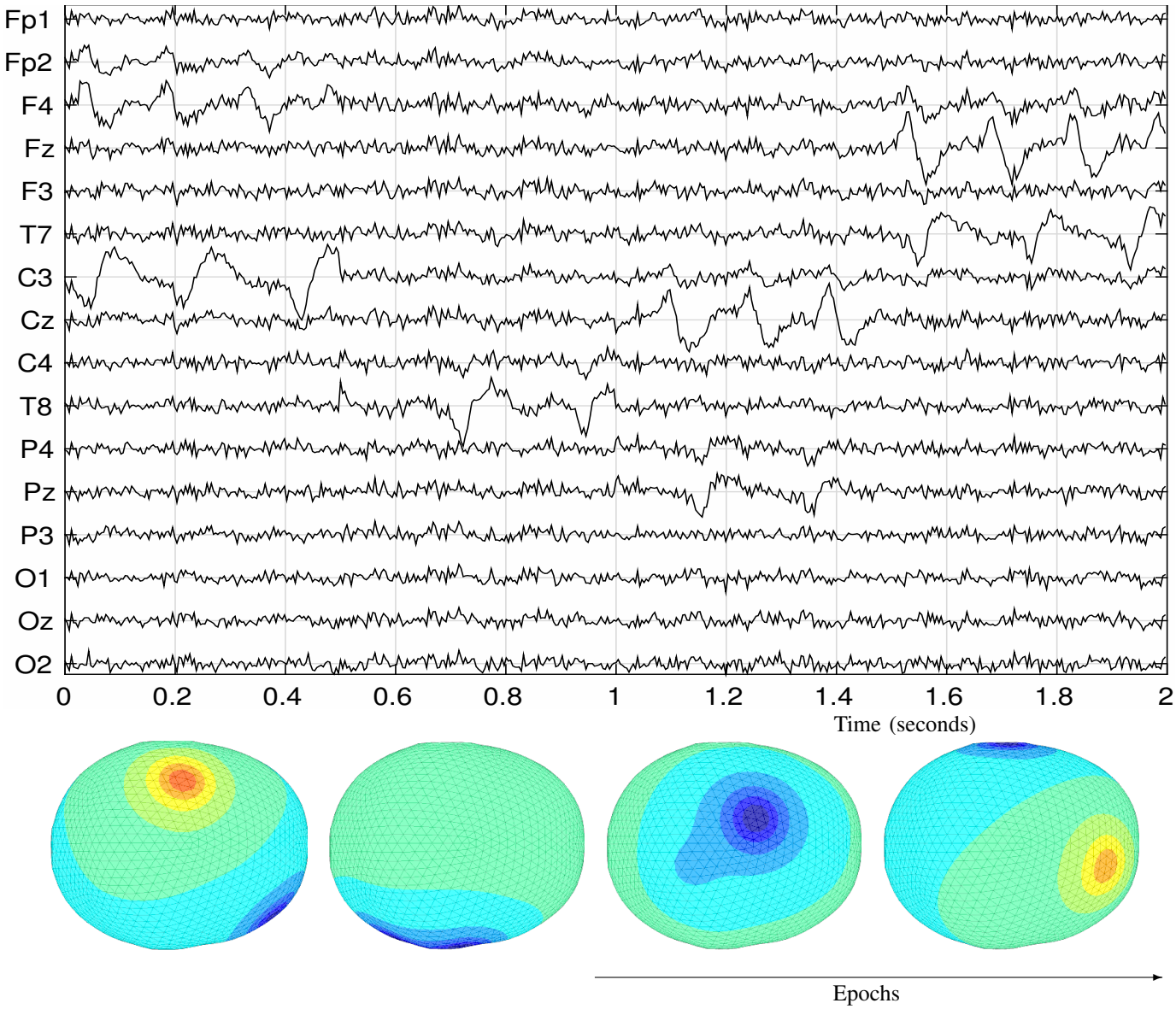

Fig. 2: An example of 2 seconds simulated EEG on 16 channels, chosen from the 128 Biosemi cap and closely matching the 10-20 system. The signals are issued from 8 non-stationary sources over 4 epochs, 2 sources active per epoch (top), with a 10dB SNR. As time goes, different locations are active, yielding distinct scalp maps (bottom).

where the number of false positives FP is divided by the total number of estimated source locations, and with the rate of true positives (TPR):

$$\mathrm{TPR} = \frac{\mathrm{TP}}{(\mathrm{TP} + \mathrm{FN})} \tag{14}$$

where the number of true positives TP is divided by the total number of simulated sources.

To measure the impact of estimated FP on overall performance, we use the relative power of the projected FP on the scalp map with respect to the power of the full estimated scalp map, computed as:

$$\mathrm{FDP} = \frac{\mathrm{P_{FP}}}{(\mathrm{P_{FP}} + \mathrm{P_{TP}})} \tag{15}$$

where $\mathrm{P_{TP}}$ and $\mathrm{P_{FP}}$ are respectively true positive and false positive projection powers. This helps in measuring the relative strength of FP values with regards to the TP source power.

We emphasize that none of the proposed metric taken individually are sufficient to evaluate the quality of the localization, *e.g.*, a low DLE might not be significant if the number of sources is over-estimated and/or if the contribution of the false positives to the estimated scalp map (FDP) is high. The localization methods will be evaluated considering these criteria altogether.

C. Results

To evaluate the advantage of using our STF dictionary, we compare with the results when using a spatial dictionary made of columns of the lead-field. SBR_w and SDMP_w denote the STF versions trying to explain the data on each individual wavelet support, while SBR_t and SDMP_t stand for those fitting the lead-field atoms on the full 2 seconds temporal windows. We also provide comparisons with two standard methods of the literature: RAP-MUSIC and FOCUSS where the same lead-field with fixed orientations is considered.

Different dictionaries were extracted after using Universal, Hysteresis and SURE threshold. The performance of SURE in terms of data reconstruction quality (GOF) was the best while Hysteresis proves to be a strong equivalent but with less coefficients.

1) Parameter sensitivity: As mentioned earlier, the two evaluated sparse algorithms have user chosen parameters, and a first brief analysis was made in order to asses their robustness to variations in these parameters. The sensitivity of the SBR method to the sparsity parameter λ is analyzed by varying it between 1% and 10% of the noise energy $\mathcal{E}_n$, *i.e.*, choosing a multiplicative factor α_n in the range [0.01 0.1] such as:

$$\lambda = \alpha_n \mathcal{E}_n \tag{16}$$

For the different SDMP versions, the key parameter is the number of desired sources N_s. As for λ, we tested different values of N_s around its true value, used in simulation.

As shown figure 3, SBR_w proves to be highly robust to the choice of λ (using equation (16)), with no significant variations of both DLE and FDP criteria with the variation of α_n. SBR_t shows a similar behavior with λ in terms of DLE, but the FDP is higher for low λ and it is consistently outperformed by SBR_w, proving the advantage of using our wavelet-based dictionary with this MP approach. When it comes to SDMP_t, an under-estimation of the number of sources highly degrades the performance in terms of localization accuracy (DLE), while an over-estimation penalizes the spurious source power (FDP). Once again one can see that for highly non-stationary sources (16 sources over 4 epochs), SBR_w constantly provides better localization accuracies while keeping low the relative power of the false detections. The SDMP_w performances are not presented here, because they are systematically much lower than those of the other three approaches, as it will be explained in the next subsection.

This analysis shows that main drawback when considering SDMP methods is that they require the number of sources as an input. Usually this parameter is deduced from a source/noise subspace analysis based on the Akaike Information Criterion or on the Minimum Description Length criterion [25]. In case of critically low SNR, synchronized sources or correlated noise, the size of the source space can be either over or under-estimated, thus considerably decreasing the performance of such methods. It is noteworthy that the same analysis applies to (RAP-)MUSIC [12]. On the other hand, SBR is much less sensitive to the choice of its λ parameter, especially when working in the wavelet domain. Indeed, by focusing on the main time-frequency components of the sources, SBR_w can easily distinguish between activities of interest and background noise.

2) Dictionary evaluation: In this section, we evaluate the performances of the different algorithms/dictionaries under their most favorable parameter choice (see previous subsection). More precisely, SDMP_t is informed with the total number of sources while SDMP_w is informed with the true number of active sources per epoch. SBR_w is applied with $\lambda_w = 0.02\mathcal{E}_n$. For SBR_t, we have chosen a value of $\lambda = 0.05\mathcal{E}_n$, which is a compromise among the λ values yielding the best results on an extended number of source and noise configurations. Besides it should be highlighted that the RAP-MUSIC is informed correctly with the true number of sources, while FOCUSS is given the true noise standard deviation.

The metrics for the two configurations are given in tables II and I. Analysing the performance per algorithm (SBR and SDMP respectively), the benefit of using such spatial-time dictionary is clearly visible for the SBR approach, where the results using the SBR_w version are consistently better. The conclusions are however the opposite for the SDMP algorithm. The bad performance of SDMP_w is due to the inherent strategy of this approach, which is forced to find a given number of sources for each wavelet support. Some sources can have negligible amplitudes for some support even in their respective active epoch, the informed number of sources being then *over-estimated*. More detailed analysis of the results show that SDMP indeed yields a high number of spurious sources (high FDR values), having a strong contribution on the estimated scalp map (high FDP values). Comparing the algorithms, the better performance of SDMP_t over SBR_t (already emphasized in [11]) can be explained by the post-processing step in the SDMP strategy, where each source position is iteratively refined. The strengths of each dictionary are revealed when used with the appropriate MP approach. In the following, we will then be comparing the STF dictionary and the spatial dictionary through the comparison of SBR_w with SDMP_t.

When it comes to highly non-stationary data with high number of sources, *i.e.*, 16 sources on 8 epochs, the SBR_w approach outperforms SDMP_t. This is especially the case when the SNR is low (3dB). Because of the thresholding, the wavelet dictionary favors the most significant temporal elements and help in distinguishing between source and noise space. SBR_w yields TDR values very close to 1, meaning that all the sources are indeed retrieved, while the FDR and the FDP values remain of the order of 0.01. Under ideal parametrization (correct N_s) SDMP_t becomes more efficient than SBR_w as the number of sources is reduced and their stationarity increases, as well as when the SNR increases. For 8 sources over 4 epochs with a SNR of $10dB$, both methods are competing with a noticeable advantage for SDMP_t when looking to the DLE. This trend is further confirmed over all the simulated configurations with less sources and epochs (*i.e.*, with more stationary and less sources, not presented here). Still, one must recall that SDMP_t performances depend on the right choice of the N_s parameter.

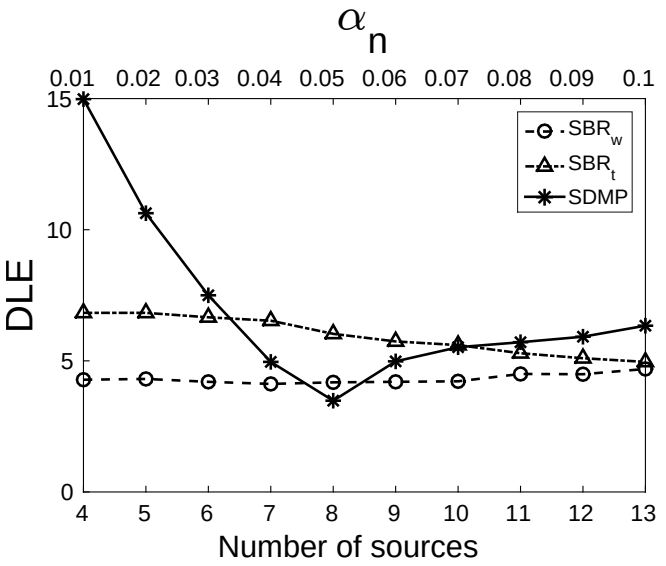

(a) DLE - 8 sources in 4 epochs

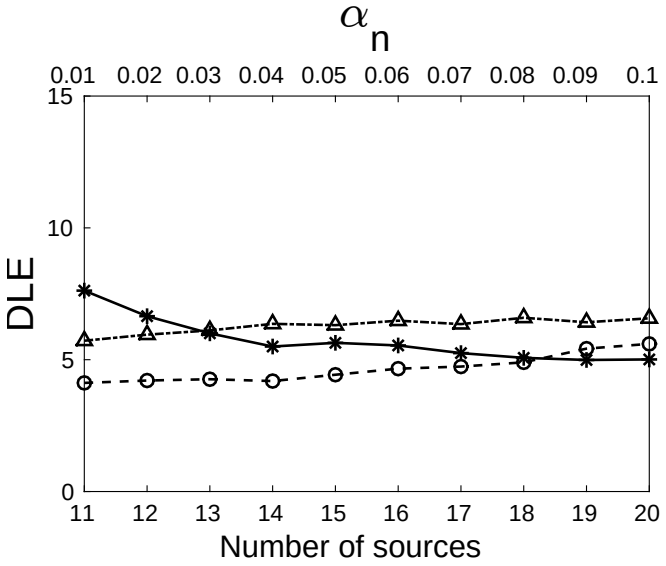

(b) DLE - 16 sources in 8 epochs

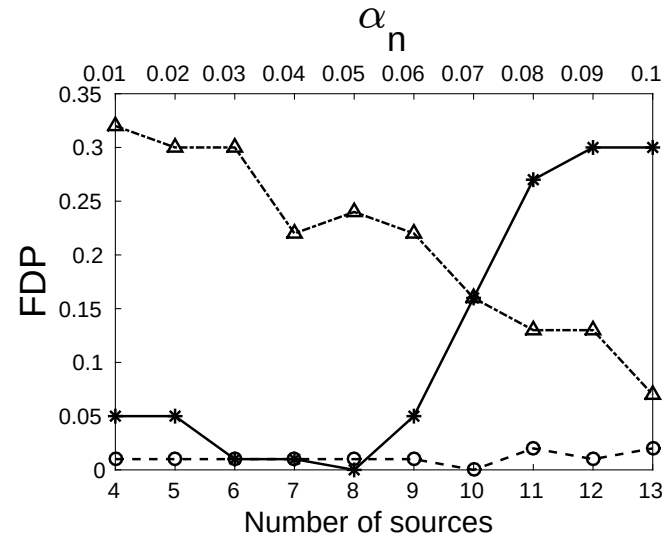

(c) FDP - 8 sources in 4 epochs

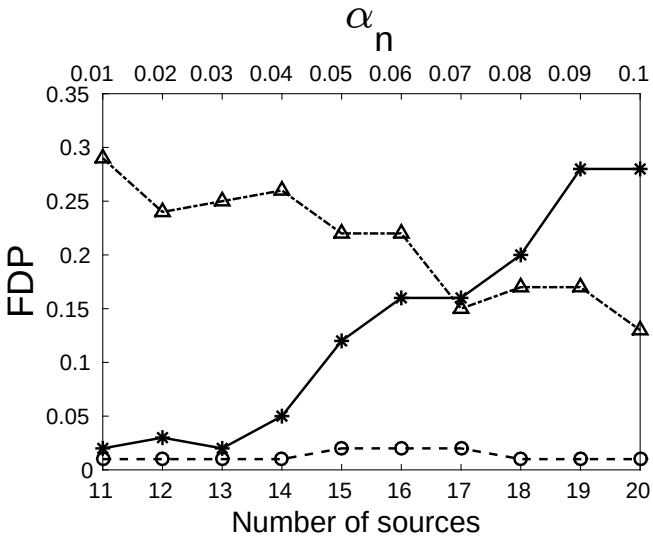

(d) FDP - 16 sources in 8 epochs

Fig. 3: Sensitivity of SBR_w, SBR_t and SDMP_t to parameter initialization, respectively to α_n fixing the λ parameter (upper axis, for SBR versions) and to the number of sources (bottom axis, for SDMP).

From an implementation point of view, the computation burden for each method show that SDMP is the most consuming method, being between 100 to 1000 times slower than SBR depending on the configurations and the dictionary used. SBR_w proves to be very robust and fast, allowing to estimate the cortical map for 2 seconds of data within about 100ms.

When it comes to standard methods of the literature, FOCUSS is less accurate when facing such non-stationary data especially for low SNR. This algorithm is to be used on longer time windows containing stationary sources, as confirmed by additional simulations. RAP-MUSIC however shows strong robustness over all the configurations.

IV. Conclusion

This paper proposes a formulation of the sparse EEG inverse problem using a data-driven space-time-frequency wavelet based dictionary. Among the optimization strategies, SBR proves to be very efficient in decomposing the data on such atoms, with high robustness to noise and to user chosen parameters while providing enhanced localization results when the non-stationarity

TABLE I: 8 sources in 4 epochs. α_{nw} = 0.01, α_{nt} = 0.05.

	TF DOMAIN		TIME DOMAIN			
10dB	SBR_w	$SDMP_w$	SBR_t	$SDMP_t$	FOCUSS	RMUSIC
GOF	**0.97**	0.89	0.92	**0.97**	0.96	0.94
DLE	4.23	11.99	6.05	**3.59**	6.88	6.42
FDP	0.02	0.13	0.23	**0.01**	0.04	0.03
TPR	**1.00**	**1.00**	0.99	0.99	0.97	0.92
FDR	**0.01**	0.38	0.14	**0.01**	0.06	0.07
Time	0.10	67.77	**0.03**	13.77	0.85	0.73
3dB	SBR_w	$SDMP_w$	SBR_t	$SDMP_t$	FOCUSS	RMUSIC
GOF	**0.90**	0.86	0.72	0.78	0.75	0.88
DLE	**5.95**	11.87	7.58	7.04	14.77	6.63
FDP	**0.01**	0.15	0.27	0.16	0.16	0.05
TPR	0.92	**1.00**	0.95	0.88	0.62	0.91
FDR	**0.01**	0.41	0.17	0.09	0.22	0.08
Time	**0.03**	81.47	**0.03**	13.63	0.75	0.73

TABLE II: 16 sources in 8 epochs. α_{nw} = 0.01, α_{nt} = 0.05.

	TF DOMAIN		TIME DOMAIN			
10dB	SBR_w	$SDMP_w$	SBR_t	$SDMP_t$	FOCUSS	RMUSIC
GOF	**0.96**	0.92	0.91	0.92	0.94	0.95
DLE	**4.37**	8.70	6.49	5.62	7.89	4.49
FDP	**0.01**	0.19	0.27	0.17	0.06	**0.01**
TPR	**1.00**	**1.00**	0.97	0.95	0.93	0.97
FDR	**0.01**	0.23	0.09	0.05	0.09	0.02
Time	0.19	31.25	**0.05**	26.03	0.80	2.39
3dB	SBR_w	$SDMP_w$	SBR_t	$SDMP_t$	FOCUSS	RMUSIC
GOF	**0.86**	0.46	0.57	0.56	0.65	0.81
DLE	**4.87**	11.17	10.25	8.22	19.13	4.92
FDP	**0.01**	0.19	0.30	0.34	0.25	0.05
TPR	0.95	**1.00**	0.72	0.85	0.46	0.96
FDR	**0.01**	0.45	0.13	0.13	0.35	0.03
Time	0.05	95.01	**0.04**	32.04	0.76	2.65

of the sources increases. As emphasized in [11], SDMP applied with a spatial dictionary is efficient when the sources are rather stationary, and if the expected number of sources is known. However it fails in decomposing the data on the proposed STF dictionary, as it requires the number of sources as an input. Sufficiently large time windows with significant activations of these sources is then needed, which is not the case when considering short time supports. Among classical approaches, RAP-MUSIC [12] provides the best accuracies, while FOCUSS needs longer time windows to provide accurate performances. This contributes to the idea that no universal localization method can cover the full spectrum of applications. Our proposed STF dictionary combined with the SBR strategy might be favored when trying to localize highly transient phenomena like epileptic spikes or cognitive evoked potential.

Using a space-time-frequency dictionary might also open interesting perspectives, as using other techniques for selecting physiologically relevant atoms instead of the wavelet denoising approach proposed in this work. For example, these atoms could be selected based on some *a priori* user knowledge, such as the frequency content for epileptic high-frequency activities [13]. Targeting the frequency band where the relevant features of the epileptic signal are lying is likely to provide enhanced localization of the epileptic sources, thus facilitating the subsequent connectivity analysis of the underlying epileptic network [9].

REFERENCES

[1] C. C. Wood, "Aplication of dipole localization methods to source identification of human evoked potentials*," *Annals of the New York Academy of Sciences*, vol. 388, no. 1, pp. 139–155, 1982.

[2] M. Scherg and D. Von Cramon, "Two bilateral sources of the late AEP as identified by a spatio-temporal dipole model," *Electroencephalography and Clinical Neurophysiology/Evoked Potentials Section*, vol. 62, no. 1, pp. 32–44, 1985.

[3] M. Scherg, "Fundamentals of dipole source potential analysis," *Auditory evoked magnetic fields and electric potentials. Advances in audiology*, vol. 6, pp. 40–69, 1990.

[4] M. Hämäläinen and R. Ilmoniemi, "Interpreting magnetic fields of the brain: minimum norm estimates," *Medical & Biological Engineering & Computing*, vol. 32, no. 1, pp. 35–42, 1994.

[5] J.-Z. Wang, S. J. Williamson, and L. Kaufman, "Magnetic source imaging based on the minimum-norm least-squares inverse," *Brain topography*, vol. 5, no. 4, pp. 365–371, 1993.

[6] W. Ou, M. S. Hämäläinen, and P. Golland, "A distributed spatio-temporal EEG/MEG inverse solver," *NeuroImage*, vol. 44, no. 3, pp. 932–946, 2009.

[7] S. J. Kiebel *et al.*, "Dynamic causal modeling for EEG and MEG," *Human brain mapping*, vol. 30, no. 6, pp. 1866–1876, 2009.

[8] B. He *et al.*, "Electrophysiological imaging of brain activity and connectivitychallenges and opportunities," *Biomedical Engineering, IEEE Transactions on*, vol. 58, no. 7, pp. 1918–1931, 2011.

[9] Y. Lu *et al.*, "Seizure source imaging by means of fine spatio-temporal dipole localization and directed transfer function in partial epilepsy patients," *Clinical Neurophysiology*, vol. 123, no. 7, pp. 1275–1283, 2012.

[10] B. He *et al.*, "Grand challenges in mapping the human brain: Nsf workshop report." *IEEE Trans. Biomed. Engineering*, vol. 60, no. 11, pp. 2983–2992, 2013.

[11] S. C. Wu and A. L. Swindlehurst, "Matching pursuit and source deflation for sparse EEG/MEG dipole moment estimation," *Biomedical Engineering, IEEE Transactions on*, vol. 60, no. 8, pp. 2280–2288, 2013.

[12] J. C. Mosher and R. M. Leahy, "Recursive MUSIC: a framework for EEG and MEG source localization." *IEEE transactions on bio-medical engineering*, vol. 45, no. 11, pp. 1342–54, Nov. 1998.

[13] Y. Lu *et al.*, "Noninvasive imaging of the high frequency brain activity in focal epilepsy patients," *Biomedical Engineering, IEEE Transactions on*, vol. 61, no. 6, pp. 1660–1667, 2014.

[14] Z. Wang *et al.*, "Single-trial evoked potential estimation using wavelets," *Computers in Biology and Medicine*, vol. 37, no. 4, pp. 463–473, 2007.

[15] A. Polonsky and M. Zibulevsky, "MEG/EEG source localization using spatio-temporal sparse representations," *Lecture notes in computer science*, pp. 1001–1008, 2004.

[16] G. Korats, R. Ranta, and S. Le Cam, "Sparse cortical source localization using spatio-temporal atoms," *Proc. Annu. Int. Conf. IEEE Eng. Med. Biol. Soc. EMBS*, pp. –, 2015.

[17] D. L. Donoho and I. M. Johnstone, "Adapting to unknown smoothness via wavelet shrinkage," *Journal of the american statistical association*, vol. 90, no. 432, pp. 1200–1224, 1995.

[18] D. L. Donoho *et al.*, "Wavelet shrinkage: asymptopia?" *Journal of the Royal Statistical Society. Series B (Methodological)*, pp. 301–369, 1995.

[19] F. Tadel *et al.*, "Brainstorm: a user-friendly application for MEG/EEG analysis," *Computational intelligence and neuroscience*, vol. 2011, p. 8, 2011.

[20] C. Soussen *et al.*, "From Bernoulli-Gaussian deconvolution to sparse signal restoration," *Signal Processing, IEEE Transactions on*, vol. 59, no. 10, pp. 4572–4584, 2010.

[21] S. G. Mallat and Z. Zhang, "Matching pursuits with time-frequency dictionaries," *Signal Processing, IEEE Transactions on*, vol. 41, no. 12, pp. 3397–3415, 1993.

[22] P. Durka and K. Blinowska, "A unified time-frequency parametrization of EEGs," *Engineering in Medicine and Biology Magazine, IEEE*, vol. 20, no. 5, pp. 47–53, 2001.

[23] Y. Pati, R. Rezaiifar, and P. Krishnaprasad, "Orthogonal matching pursuit: recursive function approximation with applications to wavelet decomposition," *Proc. 27th Asilomar Conf. Signals, Syst. Comput.*, pp. 1–5, 1993.

[24] T. Zhang, "Adaptive Forward-Backward Greedy Algorithm for Sparse Learning with Linear Models," in *Advances in Neural Information Processing Systems 21*, D. Koller *et al.*, Eds. Curran Associates, Inc., 2009, pp. 1921–1928.

[25] J. Rissanen, "Modeling by shortest data description," *Automatica*, vol. 14, no. 5, pp. 465–471, 1978.

[26] A. Cichocki, S.-i. Amari *et al.*, *Adaptive blind signal and image processing*. John Wiley Chichester, 2002.

[27] A. Antoniadis, J. Bigot, and T. Sapatinas, "Wavelet estimators in nonparametric regression: a comparative simulation study," *Journal of Statistical Software*, vol. 6, pp. 1–83, 2001.

[28] D. Donoho and I. Johnstone, "Adapting to unknown smoothness via wavelet shrinkage," *Journal of the American Statistical Association*, vol. 90, no. 432, pp. 1200–1224, 1995.

[29] R. Ranta and V. Louis-Dorr, "Hysteresis thresholding: a graph-based wavelet block denoising algorithm," *The Open Signal Processing Journal*, vol. 3, pp. 6–12, 2010.

[30] M. Stenroos, V. Mäntynen, and J. Nenonen, "A matlab library for solving quasi-static volume conduction problems using the boundary element method," *Computer methods and programs in biomedicine*, vol. 88, no. 3, pp. 256–263, 2007.

[31] H. Becker *et al.*, "A performance study of various brain source imaging approaches," in *Acoustics, Speech and Signal Processing (ICASSP), 2014 IEEE International Conference on*. IEEE, 2014, pp. 5869–5873.